IDENTIFICATION OF DRIVER GAS-ASSOCIATED Bz EVENTS AND PREDICTION OF THEIR ORIENTATION

Xuepu Zhao and J. Todd Hoeksema

Center for Space Science and Astrophysics, Stanford University
Stanford, California 94305

Abstract

An approach for identifying a driver gas-associated Bz event and its solar source is introduced. Seven newly identified events are used to further test the model developed by Hoeksema and Zhao [1991] for prediction of the magnetic orientation of some driver gas-associated Bz events from photospheric field observations. Comparison of the model predictions with observations confirms that the model may be appropriate only for those driver gas-associated Bz events which have magnetic structures lacking large internal field rotation and are associated with active region-CMEs.

1. Introduction

We have developed a model [Hoeksema and Zhao, 1991, hereafter referred to as paper 1] to predict the direction of driver gas-associated Bz events from the computed coronal magnetic field orientation above the solar event site. Observations of the photospheric field at the National Solar Observatory provide the input for the model. The comparison of predictions of the model with in situ observations of four $-$Bz events showed that the magnetic field orientations can only be predicted by the model for driver gas associated with the active region(AR)-CMEs. With such a limited number of cases, the results are only suggestive, but they show that it is worth pursuing further the hypothesis. The purpose of the present work is to find more driver gas-associated Bz events with identifiable source regions and to further test the model with these newly detected events.

2. Identification of a Driver Gas-Associated Bz Event and Its Solar Source

We define a Bz event as an interval when the magnitude of the north-south component of the interplanetary magnetic field observed at 1 AU is greater than 10 nT for more than 3 hours. 54 such events have been identified using the Omnitape data set between 1978 and 1982. Of these, 28 events were preceded by shocks and 26 events lacked a shock association.

We explicitly assume that a Bz event preceded by a shock is driver gas-associated if it occurred in an interval when a bidirectional electron heat flux event (BDE) or a bidirectional low-energy proton event (BDP) was observed. The tabulations of BDEs [Gosling et al., 1987, 1990] and BDPs [Marsden et al., 1987] show that sixteen ot the events were associated with driver gas. The four $-$Bz events observed between 1978 and 1979 are the same as those detected by Tsurutani et al [1988] on the basis of a full complement of solar wind and magnetic field data from ISEE-3. and have been analyzed in paper 1.

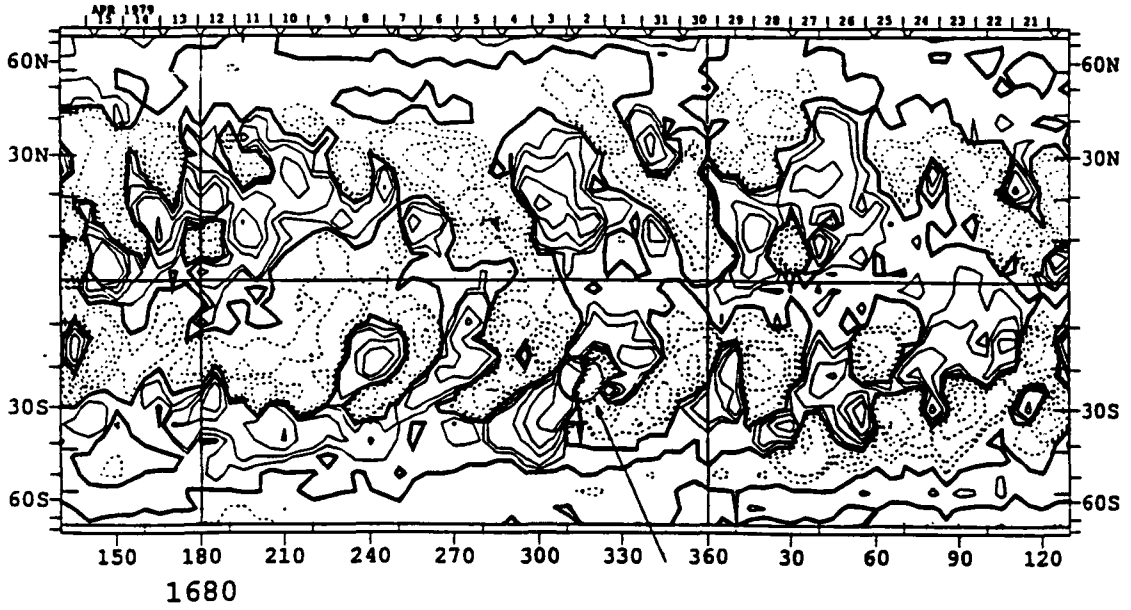

Figure 1. The National Solar Observatory synoptic chart of the photospheric magnetic field with the 1979/04/03 01:09 (S26 W14) AR-associated CME centered. The field has been averaged into 30 bins of sine latitude from north to south each 5 Carrington degrees. The photosphere is shown in an equal area projection (equal steps in sine latitude). The bottom axis shows the Carrington longitude, while the top axis is labeled by central meridian passage date. The center of small circle denotes the location of the flare associated with the CME and Bz event. The tip on the small circle denotes the orientation of Earth's rotation axis when the flare occurred.

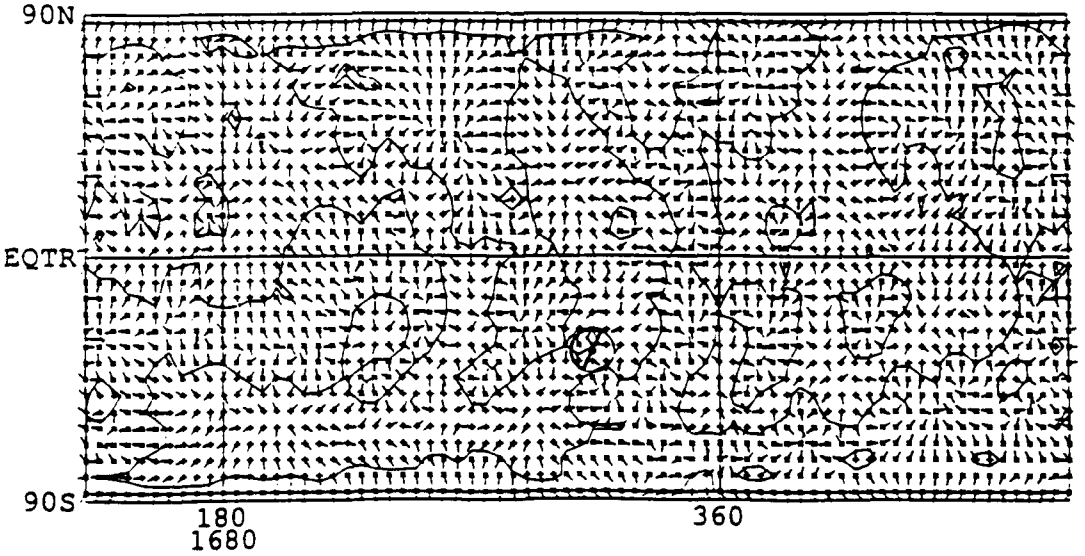

Figure 2. Predicted the magnetic orientation at 1.03 $R_{\odot}$. The small circle and the thick arrow have the same meaning as in Figure 1.

To identify the solar source of a driver gas-associated Bz event, we compared the Sun-Earth travel time computed from the observed velocity of the driver gas with the elapsed time between the associated solar parent event and the onset of the driver gas for each of the five events analyzed in paper 1. The variations in these values suggest uncertainties of ± 12 hours in the computed Sun-Earth travel time for AR-CME associated events and ± 24 hours for quiescent promionence(QP)-CME associated events (see Table 1). By examing the SMS-GOES X-ray data (Solar–Geophysical Data comprehensive reports) and the catalog of solar (quiescent) filament disappearances [Wright, 1991] we identified, of the twelve driver gas-associated Bz events not previously analyzed, only seven having one or more candidate solar parents within the time window.

3. Model and Method of calculation

It is now widely believed that the energy released in the CME process comes from the surplus magnetic energy which is in excess of the energy of the potential field [e.g., Low, 1990]. Thus the internal magnetic field of a CME during the initial phase, when the surplus magnetic energy starts to release, must be nonpotential. How is the field configured during the late phase of the CME when liberation of the excess "free" magnetic energy ends? Observations of the interplanetary disturbances may provide some insight into this matter. Marubashi [1986] has shown that interplanetary magnetic structures with large internal field rotation, such as some "magnetic clouds," can be described by a constant α force-free field and are associated with erupting (quiescent) prominence-CMEs. He inferred that many magnetic clouds are extended or propagated through interplanetary space with their configurations almost unchanged. This implies that the internal fields for QP-CMEs are nonpotential during the late phase. On the other hand, in situ observations also show the existence of magnetic structures lacking large internal field rotation, such as "magnetic bottles" [Gosling et al., 1987] or "Planar Magnetic Structures" (PMS) [Nakagawa et al., 1989]. Such structures may be inferred to have a nearly current-free field [see paper 1]. Thus if the magnetic structure is convected by the solar wind into interplanetary space with its configuration maintained, the internal field of the associated CME must also be potential during the late phase. This may validate the use of the potential field model for predicting the field configuration in AR-CMEs.

Here we calculate the orientation of the coronal field above a parent event site including the effects of solar wind outflow and neighboring regions. We use the source surface potential field code with the source surface located at 2.5 $R_\odot$ [Hoeksema et al., 1982,1983; Hoeksema, 1984]. The field at the release height is calculated using the synoptic chart of the line-of-sight photospheric magnetic field as an inner boundary condition. The contour map in Figure 1 shows the photospheric line-of-sight magnetic field over the entire Sun. The center of the small circle shows the the location of the flare that occurred at S26° W14° on April 3, 1979, 01:09 UT. This flare, accompanied by a M4 soft X-ray event, is associated with the CME that produced the driver gas which caused the northward Bz event observed near Earth by ISEE-3 on April 5,1979.

As discussed in paper 1, the driver gas creating the coronal and interplanetary shocks approaches a constant velocity in the late phase of the CME. For convenience we call the height where the front of CMEs ceases to accelerate the "release height". The release heights for AR-CMEs are less than or equal to 1.2 $R_\odot$. We selected 1.03 $R_\odot$ and 1.20 $R_\odot$ as the candidate release heights (see paper 1). Figure 2 shows the field direction at 1.03 $R_\odot$

computed from the photospheric field displayed in Figure 1. Figure 2 shows that the field has a northward component at 1.03 $R_\odot$ above the parent event site. Harrison [1986] found that flare-associated CMEs appeared to leave the solar surface during weak soft X-ray bursts, preceding the associated flares by tens of minutes. The precursor X-ray brightenings had a large spatial scale size, $\sim 10^5$ km, and the resulting flares were positioned near one leg of the angle subtended by the CME. To search for the dominant polarity in the area covered by the soft X-ray bursts, we drew a thick 10^5 km radius semicircle centered at the parent event site extending across the polarity inversion line (see Figures 1 and 2). For this event the dominant transverse field in the thick semicircle is directed north (N) with respect to the Earth's rotation axis, consistent with the observed magnetic orientation in the Bz event (See event #2 in Table 2).

Table 1: Sun-Earth Travel Time

Bz Event Onset t_b	Parent event Onset t_p	t_b-t_p dt1 (hrs)	Velocity of Driver gas km/s	Sun-Earth Travel time dt2 (hrs)	dt2-dt1 (hrs)
1978/08/27 23:00	1978/08/23 12:00±4:00 (DF)	107	450	92	-15±4
1978/09/29 07:00	1978/09/27 14:00	41	890	47	5
1979/04/03 21:00	1979/03/31 21:00	72	555	75	3
1980/12/19 12:00	1980/12/16 *10:00*	74	550	75	1
	1980/12/16 12:00	72			3
	1980/12/16 15:00	69			6
1981/04/12 23:00	1981/04/10 12:00	59	670	62	3
	1981/04/10 17:00	54			8
	1981/04/10 20:00 (DF)	51			11

Table 2: Observation and Prediction

ID Number	Bz Event UT	Driver Gas UT	NERA	Solar Source Onset Location	Field Orientation 1.03	Field Orientation 1.20
#1	2908-2920 March 1979 (southward)	2908-2915 March 1979 (BDE)	-26°	1979/03/25 21:19 S29 E48	SW	W
				1979/03/26 11:50 N05 W78	N	NW
#2	0510-0514 April 1979 (northward)	0510-0605 April 1979 (BDE) 0518-0613 April 1979 (BDP)	-26°	1979/04/03 01:09 S26 W14	N	NE
#3	1916-2005 March 1980 (northward)	1921-2002 March 1980 (BDP) 1916-2119 March *1980* (Cloud)	-25°	1980/03/16 06:30 N36 E04	NW	N
#4	2523-2604 July 1981 (southward) 2607-2610 July 1981 (northward)	2519-2618 July 1981 (BDE) 2522-2605 July 1981 (BDP)	8°	1981/07/23 23:06 RS10 E55	SW	W
#5	2210-2221 Oct. 1981 (southward)	2207-2214 Oct. 1981 (BDE)	26°	1981/10/19 13:18 N20 E20	SW	W
#6	1200-1210 Feb. 1982 (northward) 1222-1317 Feb. 1982 (southward)	1200-1206 Feb. 1982 (BDP) 1203-1317 Feb. 1982 (Cloud)	-16°	1982/02/09 04:10 S12 W90	SE	S
				1982/02/09 13:15 S10 E06	N	NW
#7	2508-2511 April 1982 (southward)	2510-2709 April 1982 (BDE) 2600- > 2618 April 1982 (BDP)	-25°	1982/04/22 14:54 N14 E48	SE	E

4. Prediction and Conclusion

The computed magnetic-field orientation at the location of the candidate parent events for each of the seven Bz events at the altitudes 1.03 $R_\odot$, and 1.20 $R_\odot$ are shown in Table 2.

The first and second columns of Table 2 list the days and hours during which the Bz events and the gas driving interplanetary shocks were observed. The magnetic orientation of the Bz events in GSM coordinate system and the characteristics of the driver gas are shown in

parentheses in the first and second columns, respectively. The 24-hour average position angle of the north extremity of the Earth's rotation axis at the time of the parent event is listed in the third column. The next columns under the title of Solar Source show the candidate solar sources of the Bz events and the predicted magnetic orientations at two possible release heights. We assigned each event to one of eight 45 degree sectors, N, NW, etc. relative to the Earth's rotation axis. For example, the second event (#2) from Table 2 occurred between 10 UT and 14 UT, April 5, 1979, was directed northward, and overlapped in time with the bidirectional electron event and bidirectional proton event observed, respectively, in the intervals of April 5, 10 UT – April 6, 05 UT and April 5, 18 UT – April 6, 13 UT, 1979. The associated AR-CME occurred on 01:09 UT, April 3, 1979 at the disk position of S26° W14°. The position angle of the north extremity of the Earth's rotation axis at the onset of the flare is −26°.

Five Bz events in Table 2, viz. #2, #3, #4, #5 and #7, are associated with single candidate AR-CMEs. The remaining two events (#1 and #6) have two candidate AR-CMEs. It is seen from Table 2 that the prediction of magnetic orientation at 1.3 $R_\odot$ for events #2, #3, #5 and #7 is consistent with that of the observed Bz events. As shown in paper 1, because the release height for AR-CMEs is usually less than 1.20 $R_\odot$, not all predictions at 1.20 $R_\odot$ are consistent with interplanetary observations. Event #4 consists of a southward and a northward Bz event separated by a interval of 3 hours. The associated BDE covers both southward and northward subevents. Thus it is probably a structure with large internal field rotation that can not be described by the potential model. For the remaining two events, we can infer nothing because both northward and southward field components are predicted and we cannot determine which is the true solar source of the Bz event. However, if our hypothesis is true, we can predict which event is the solar source.

In summary, we have now identified 7 driver gas associated Bz events for which the solar source can relatively confidently be identified as an AR-CME. In each case the north-south component of the coronal field direction computed at 1.03 $R_\odot$ using the potential field model agrees with the Z component of the IMF observed by spacecraft at 1 AU. These results show that the assumption made in paper 1, that the excess magnetic energy associated with coronal currents is transferred totally to other forms of energy during the late phase of magnetic energy release, may be proper for the AR-CMEs. The model developed in paper 1 may be used to predict the magnetic-field orientation of interplanetary north-south IMF events associated with interplanetary magnetic structures lacking large internal field rotation and with AR-CMEs.

Acknowledgement.

We thank P. Scherrer for helpful discussions, T. Bai for providing his catalog of major flares and J. Harvey for providing data from the National Solar Observatory. The Omnitape of interplanetary medium data is provided by the National Space Science Data Center. This work was supported in part by the Office of Naval Research under Grant N00014-89-J-1024, by the National Aeronautics and Space Administration under Grant NGR5-020-559, and by the Atmospheric Sciences Section of the National Science Foundation under Grant ATM90-22249.

REFERENCES

Gosling, J. T., Coronal mass ejections and magnetic flux ropes in interplanetary space, in *Physics of Magnetic Flux Ropes* ed. by C. T. Russell, E. R. Priest, L. C. Lee, pp. 343–364, American Geophysical Union, Washington DC, 1990.

Gosling, J. T., D. N. Bakes, S. J. Bame, W. C. Feldman, and R. D. Zwickl, Bidirectional solar wind electron heat flux events, *J. Geophys. Res., 92*, 8519–8535, 1987.

Gosling, J. T., S. J. Bame, D. J. McComas, and J. L. Phillips, Coronal mass ejections and large geomagnetic storms, *Geophys. Res. Lett., 17*, 901–904, 1990.

Harrison, R. A., Solar coronal mass ejections and flares, *Astron. Astrophys., 162*, 283–291, 1986.

Hoeksema, J. T., Structure and Evolution of the Large Scale Solar and Heliospheric Magnetic Fields, thesis, Stanford University, CSSA-ASTRO-84-07, 1984.

Hoeksema, J. T., J. M. Wilcox, and P. H. Scherrer, Structure of the heliospheric current sheet in the early portion of sunspot cycle 21, *J. Geophys. Res., 87*, 10331–10341, 1982.

Hoeksema, J. T., J. M. Wilcox, and P. H. Scherrer, Structure of the heliospheric current sheet: 1978–1982, *J. Geophys. Res., 88*. 9910–9920, 1983.

Hoeksema, J. T. and Xuepu Zhao, Prediction of magnetic orientation in driver gas-associated $-$Bz events, *J. Geophys. Res.*, in press, 1991.

Kahler, S., Coronal mass ejections, *Rev. Geophys., 25*, 663–675, 1987.

Low, B. C., Equilibrium and dynamics of coronal magnetic fields, *Annu. Rev. Astron. Astrophys. 28*, 491–524, 1990.

Marubashi, M., Interplanetary magnetic clouds and solar filaments, *Adv. Space Res., 6*, 335–344, 1986.

Marsden, R. G., T. R. Anderson, C. Tranquille, K.-P. Wenzel, and E. J. Smith, ISEE 3 observations of low-energy proton bidirectional events and their relation to isolated interplanetary magnetic structures, *J. Geophys. Res., 92*, 11,009–11,019, 1987.

Nakagawa, T., A. Nishida and T. Saito, Planar magnetic structures in the solar wind, *J. Geophys. Res., 94*, 11,761–11,775, 1989.

Tsurutani, B. T., W. D. Gonzalez, F. Tang, S.-I. Akasofu, and E. J. smith, Origin of interplanetary southward magnetic field responsible for major magnetic storms near solar maximum (1978–1979), *J. Geophys. Res., 93*, 8519–8531, 1988.

Wright, C. S., *Catalog of Solar Filament Disappearances 1964–1980*, REPORT UAG-100, National Geophysical Data Center, 1991.